Behavior and Response of Headed Stud Connectors in Composite Steel Plate Girder Bridges under Cyclic Lateral Deformations

HAMID BAHRAMI, ERIC V. MONZON, AHMAD M. ITANI and IAN G. BUCKLE

ABSTRACT

Most of the mass of steel plate girder bridge superstructures is concentrated in the reinforced concrete deck. During a seismic event, the inertia force that is generated in the reinforced concrete deck is transferred to the support cross frames through the headed stud connectors. Seismic analyses showed that these connectors are subjected to combined axial tension and shear forces. If not designed properly, these connectors may fail prematurely during an earthquake, altering the load path and subjecting other bridge components to forces they are not designed for. To verify these observations, two half-scale models of plate girder bridge subassembly were constructed and subjected to cyclic testing. The two specimens represented two different configurations of headed stud connectors in transferring the deck seismic forces. The connectors in the first specimen connected the girder top flange to the reinforced concrete deck, while the connectors in the second specimen connected the cross-frame top chord to the deck. These experiments showed that the connectors were indeed vulnerable under transverse lateral loading. The failure mode of these connectors is a combination between shear and tensile forces or concrete breakout. Based on this investigation, design equations were proposed and adopted in the AASHTO LRFD Bridge Design Specifications to evaluate the resistance of such connectors under shear and tensile forces.

Keywords: stud connectors, seismic design, steel plate girders, reinforced concrete deck, steel girder bridge.

INTRODUCTION

Composite steel plate girder bridge superstructures have experienced various degrees of damage during recent earthquakes. This damage has occurred in plate girders, reinforced concrete decks, stud connectors, bearings, cross frames and their connections. In 1992, a series of three earthquakes with a maximum magnitude of 7.0 occurred near the town of Petrolia in northern California (Caltrans, 1992). Some notable damage was reported to the Van Duzen River Bridge, which has a steel plate girder superstructure. The support cross frames and the lateral bracing of the southbound bridge experienced buckling and yielding. In addition, the reinforced concrete deck experienced damage to the stud connectors at one of the abutments. This damage showed that the stud connectors, used to achieve a composite action between the steel plate girders and the concrete deck, were subjected to seismic forces for which they were not designed.

Earthquake loading in the lateral direction of the bridge causes transverse bending of the superstructure, resulting in seismic reactions at abutments and piers. The majority of the seismic inertia loads in steel plate girder bridges are generated in the reinforced concrete deck because it accounts for almost 80% of the superstructure weight. Carden, Itani and Buckle (2005) showed that the stud connectors between the deck and girders are among the critical components in the seismic transverse load path. However, very limited research is available on the response and the resistance of these connectors in transferring these seismic forces. With the absence of such critical information, it is commonly assumed that the stud connectors, designed for strength and fatigue, are adequate for seismic forces. The observed damage, however, raised concerns about the adequacy of these connectors in transferring the seismic forces to the supports and showed the need to better understand their response under seismic loading.

Most of the research conducted on stud connectors was to investigate the composite action between steel girders and reinforced concrete deck. Ollgaard, Slutter and Fisher (1971), Oehlers and Johnson (1987), Lloyd and Wright (1990) and Oehlers (1995) have studied the shear resistance of connectors in composite beams. Hawkins and Mitchell (1984), Gattesco and Giuriani (1996), and Seracino, Oehlers

Hamid Bahrami, Former Doctoral Student, Department of Civil and Environmental Engineering, University of Nevada, Reno, NV 89557

Eric V. Monzon, Assistant Professor, Department of Civil Engineering, West Virginia University—Institute of Technology, Montgomery, WV (corresponding author). Email: evmonzon@gmail.com

Ahmad M. Itani, Professor, Department of Civil and Environmental Engineering, University of Nevada, Reno, NV. Email: itani@unr.edu

Ian G. Buckle, Professor, Department of Civil and Environmental Engineering, University of Nevada, Reno, NV. Email: igbuckle@unr.edu

Paper No. 2013-28

and Yeo (2003) reported strength and stiffness degradation in the concrete around the connectors due to unidirectional cyclic loadings. McMullin and Astaneh-Asl (1994) recommended a cone be placed around connectors to create ductile response and to avoid brittle fracture. Mouras et al. (2008) investigated the axial resistance of the stud connector under static and dynamic loading. They showed experimentally that the limiting factor in transferring the in-plane moment capacity of a reinforced concrete deck is the axial resistance of connectors. They have also shown that the standard haunch detail in steel plate girders lowers the tensile resistance of stud connector and offers limited ductility because that zone is not adequately reinforced.

SEISMIC DEMAND ON STUD CONNECTORS IN A COMPOSITE-PLATE GIRDER BRIDGE

A 3D finite element model of a steel plate girder superstructure was developed to determine the forces on stud connectors under seismic loading. The geometry of this superstructure was taken from a bridge designed by Caltrans engineers and used in their Bridge Design Practice for training purposes (Caltrans, 2007). The composite steel plate girder bridge consists of three continuous spans. The total length of the bridge is 385 ft, with span lengths of 110, 165 and 110 ft. The total width of the bridge is 58 ft, which consists of five steel plate girders spaced at 12 ft. The reinforced concrete deck is 9⅛ in. thick. All intermediate cross frames are spaced at 27.5 ft and consist of chevron-bracing members with single L4×4×5⁄16 sections connected to the bottom chord of double L6×6×½. The support cross frames have an X-pattern using single L4×4×½ sections that are interconnected at their mid-length where the diagonals cross. Stud connectors were used throughout the length of the bridge. These connectors were designed for strength and fatigue according to the AASHTO LRFD Bridge Design Specifications (AASHTO, 2008). At the positive moment regions, three ⅞-in.-diameter, single-headed stud connectors spaced at 15 in. were used on top of each girder. In the negative moment region, the connectors were spaced at 24 in. The transverse spacing between the connectors is 3 in. Elastomeric bearings with transverse shear keys were used at the abutment and at the piers.

The SAP2000 computer program was used in the analytical investigation (CSI, 2010). The steel girders, stiffeners and decks were modeled using shell elements, while the intermediate and support cross frames were modeled using frame elements. The support cross frames were modeled using nonlinear link elements with multilinear plastic Takeda hysteretic properties. Vertical and rotational springs were used at the supports to model the vertical and rotational stiffness of the elastomeric bearings. The elastomeric bearing stiffness properties that were included in the analytical model are shown in Table 1. The stud connectors were modeled using linear link elements. Their stiffnesses were calculated based on the equations proposed by Carden et al. (2005). For each stud connector, the lateral and axial stiffnesses are equal to 500 kip/in. and 1000 kip/in., respectively. The overall view of the SAP2000 model is shown in Figure 1. It is assumed in the model that the substructure is rigid because the purpose of this analysis is to determine the distribution of seismic forces among the shear connectors. Although the substructure flexibility affects the global seismic response, it does not affect the lateral load path in the superstructure.

The total seismic weight of the superstructure is 3407 kips. Dead load analysis showed that each abutments carries 331 kips, while the intermediate supports carry 1372 kips each. Table 2 shows the periods and modal participating mass ratios of the first nine modes from modal. The longitudinal and transverse directions correspond to the global x- and global y-direction in the model.

The seismic demands on the reinforced concrete deck and the stud connectors were determined using nonlinear pushover analysis.

The pushover analysis was performed using a mode 5 load pattern because it was the dominant transverse mode, with 79% mass participation in that direction, as shown in Table 2. The deformed shape of the girders is shown in Figure 2. Figure 3 shows the vertical deformation contours of the reinforced concrete deck, which clearly indicates a torsional rotation of the superstructure about its longitudinal axis. This implies that the stud connectors are subjected to axial forces in addition to shear forces in order to maintain deformation compatibility between the reinforced concrete deck and the steel plate girders.

Figure 4 shows the schematic view of the stud connectors on the top flange of the plate girders. Connector 2 is the middle connector and is located along the plane of girder web while connectors 1 and 3 are the exterior connectors. The seismic force demands on the stud connectors from the nonlinear response history analysis are shown in Figure 5. In this figure, P represents axial force in the connectors, VL is the shear force in longitudinal direction and VT is the shear force in transverse direction. The numbers that follow the aforementioned letters refer to the connector number. Figure 5a shows the axial force distribution in each of the connectors on girder 1 along the length of the bridge superstructure at 5% drift (drift is ratio of relative girder displacement to the girder height). This plot shows that the transverse seismic force creates large axial force demands on the connectors directly over the supports (abutments and bents). The middle connector shows minimal axial force while the connectors on either side are subject to equal and opposing axial forces. Figure 5b shows the longitudinal shear force distribution in the connectors in girder 1. The distribution indicates force transfer between the reinforced concrete deck and steel girders as the composite section resists the

Table 1. Elastomeric Bearing Properties		
Location	**Vertical Stiffness (kips/in.)**	**Rotational Stiffness (kips-in./rad)**
Abutments	3,284	64,650
Piers	6,829	225,000

Table 2. Modal Periods and Mass Participation Ratios			
Mode No.	**Period (sec)**	**Mass Participating Ratio**	
		UX (%)	**UY (%)**
1	4.176	100	0
2	0.384	0	0
3	0.380	0	0
4	0.208	0	0
5	0.202	0	79
6	0.186	0	3
7	0.143	0	0
8	0.113	0	15
9	0.084	0	0

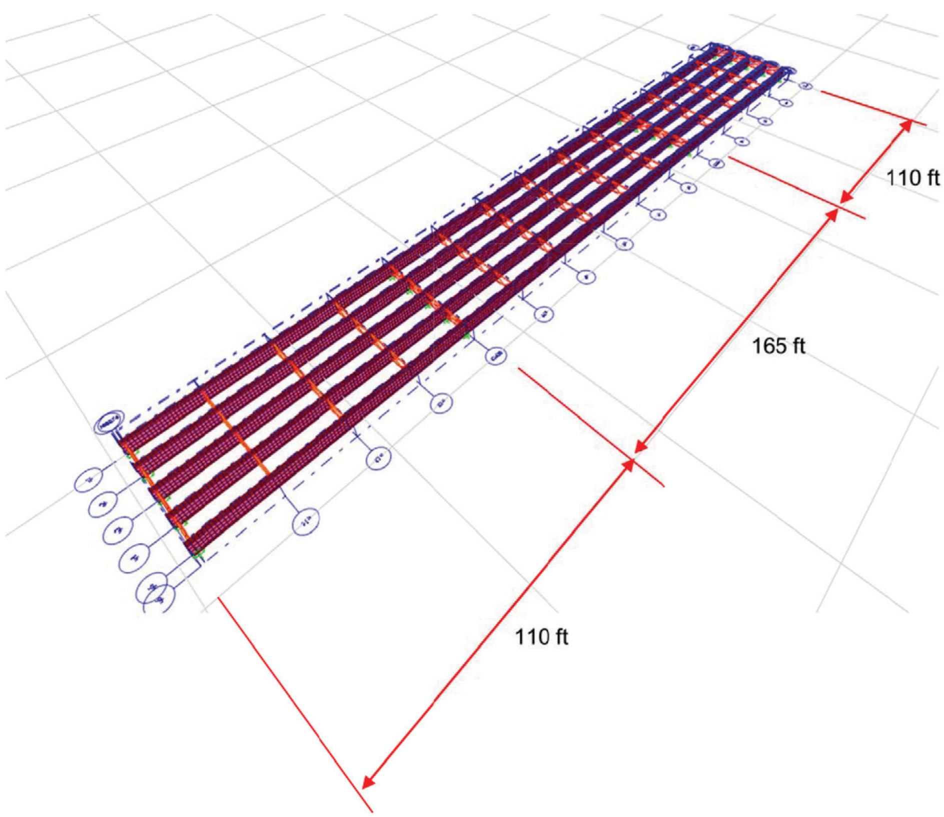

Fig. 1. Finite element model of three-span five-girder bridge (deck is not shown for clarity).

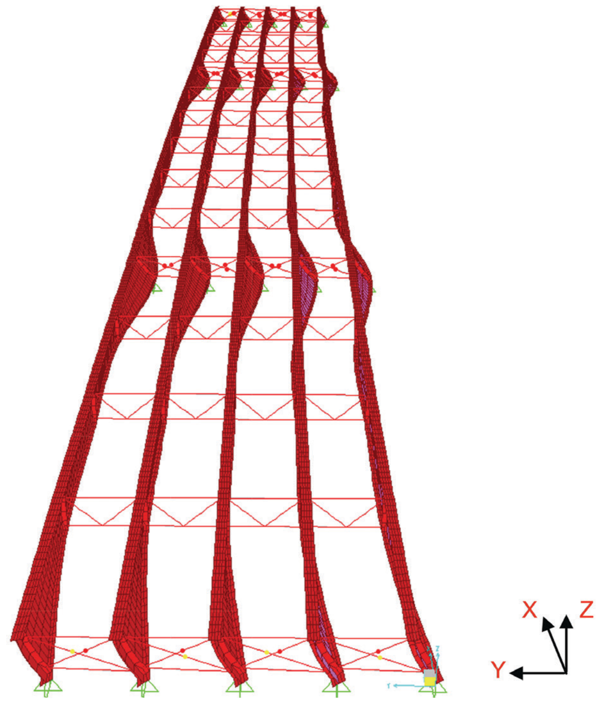

Fig. 2. Deformed shape of the superstructure (deck not shown for clarity).

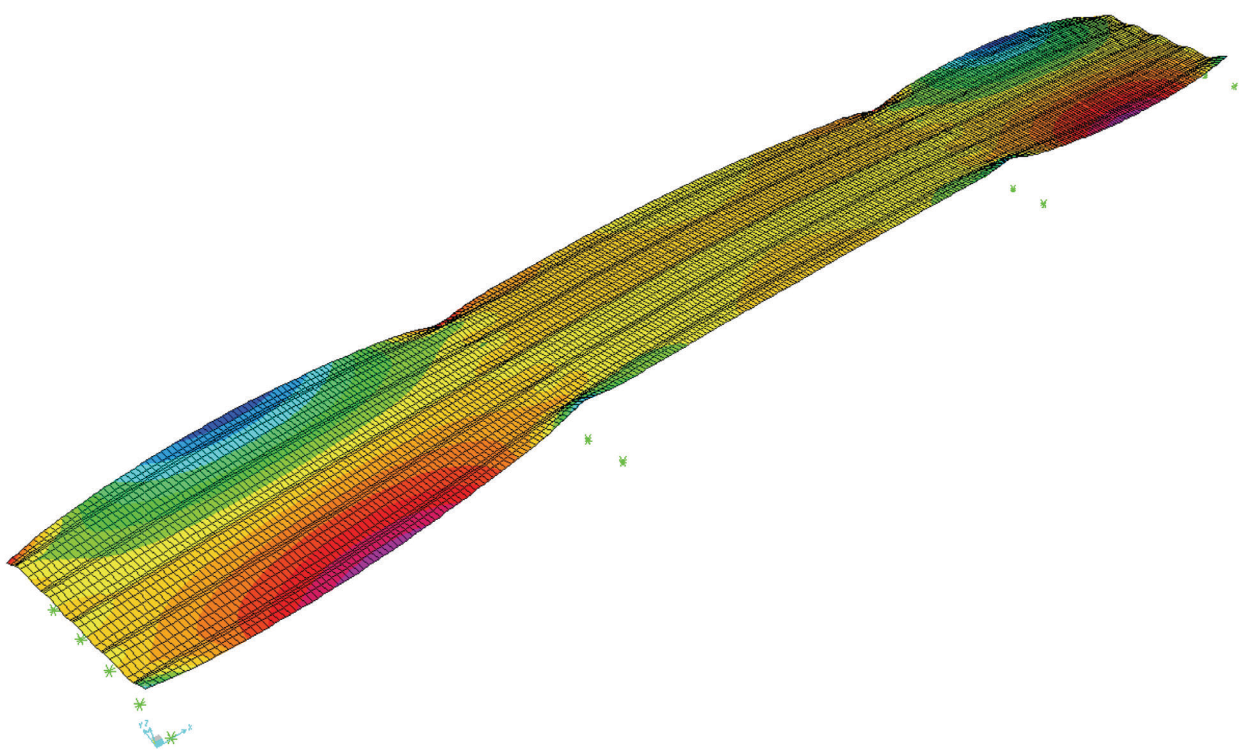

Fig. 3. Contour of deck vertical deformation during the pushover analysis.

transverse seismic forces through bending in the plane of the deck. Figure 5c shows the transverse shear force distribution in the connectors in girder 1. This distribution is the result of combined transverse shear force transfer between the reinforced concrete deck and steel girders and torsional moment on the superstructure. The torsional moment causes out-of-plane bending in deck. The bending moment results in equal and opposite transverse shear forces in the connectors on either side of the girder. These opposing forces cancel out once all the forces in a row of connectors are summed up, as shown in Figure 5d. The high peaks near the supports indicate significant force transfer between the reinforced concrete deck and steel girders. The other small peaks seen in this plot are at the location of intermediate cross frames. This shows that the intermediate cross frames attract only a small amount of the transverse seismic forces.

The significant observation from this analysis is that the stud connectors in a composite steel plate girder superstructure not only resist shear in the longitudinal direction, but also experience significant axial and transverse shear forces during a seismic event. With peaks occurring near the supports, the connection of the reinforced concrete deck via a stud connector to the top flange of the girder may be vulnerable in these regions and should be designed for the seismic forces. The large peaks in the plots for the connector forces clearly surpass the elastic range for these connectors, which indicate damage to the connection between the reinforced concrete deck and the steel plate top flange. Any nonlinearity in the connectors near the supports will lead to redistribution of the forces in the connectors in their vicinity, which in turn will translate into a damaged zone (over a certain distance) near the supports. Failure of the stud connectors at and near the supports will alter the lateral load path. The deck seismic forces will be transmitted to the stud connectors that are located at some distance from the support, which are then transferred to the girders and then to the bearings and substructure. The girders, in this situation, are subjected to bending about their weak axis, which could damage the girders.

The seismic force demands on the connectors at support locations is illustrated in Figure 6a. The axial tensile force in the connector is transferred from the reinforced concrete deck through a cone, as illustrated in Figure 6b. Based on these observations, experimental investigation was performed to better understand and verify the response of stud connectors under this complex loading.

EXPERIMENTAL INVESTIGATION

Two half-scale test specimens representing the subassembly system of reinforced concrete deck, top and bottom chords and steel girders were constructed and subjected to cyclic lateral loading. The test specimens used in the experimental program represented a 3-ft-long slice of a three-girder

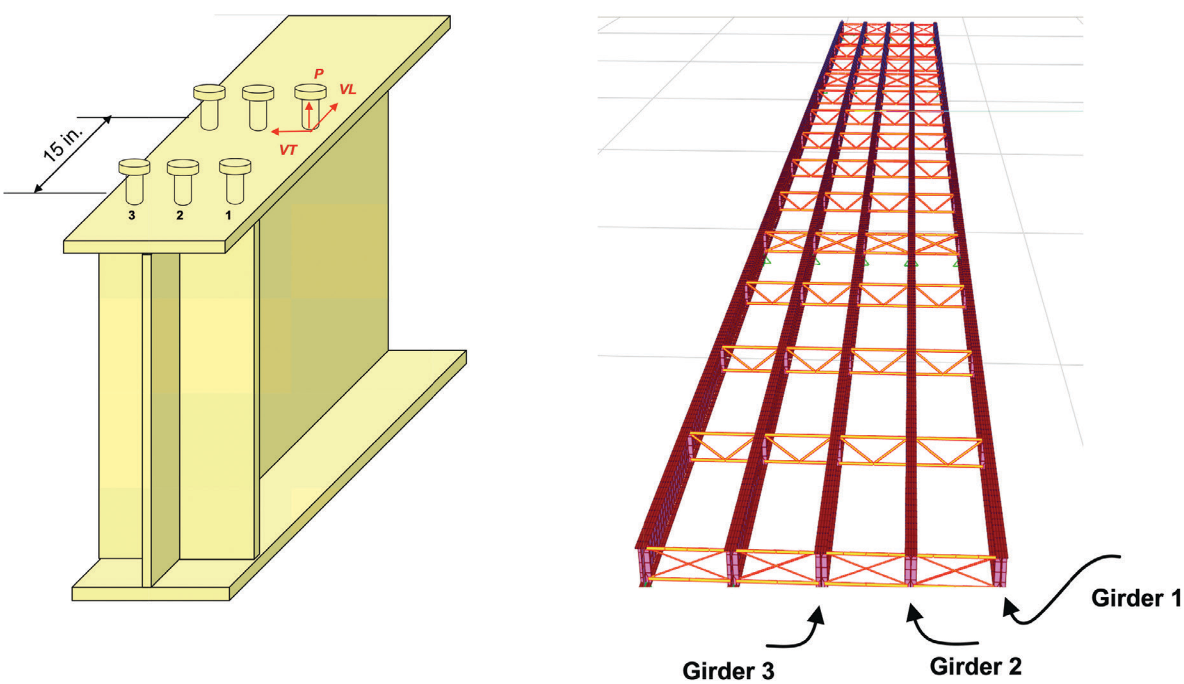

(a) (b)

Fig. 4. (a) Schematic view of stud connectors; (b) location of girders.

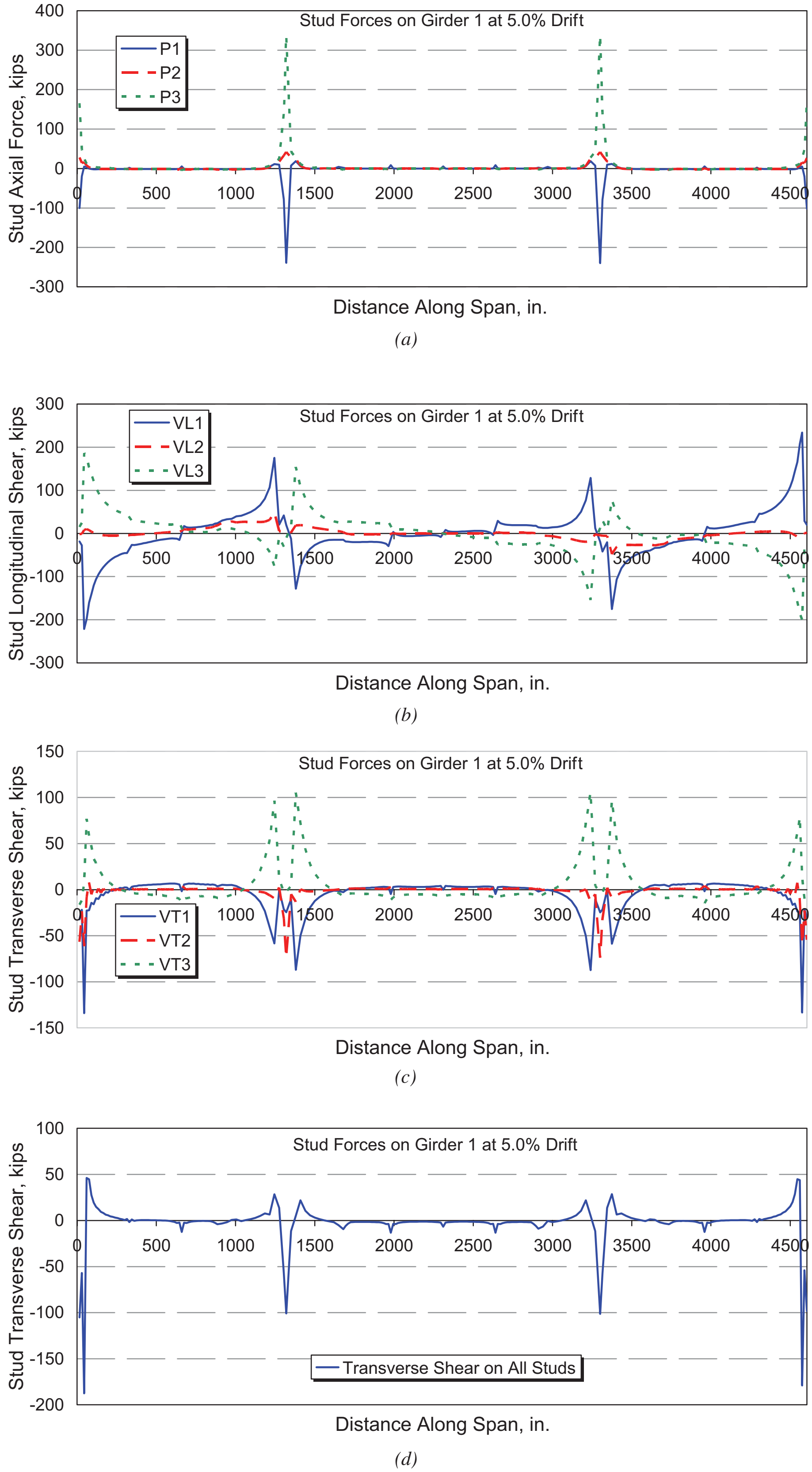

Fig. 5. Stud connector force distribution in girder 1 at 5% superstructure drift.

bridge superstructure over an intermediate bent. The overall dimensions of the specimens were scaled down to 50% from the prototype bridge cross-section discussed in the analytical program.

The test specimens represented two different configurations of transferring the deck seismic forces to the bearings and the substructures. Neither specimen had any diagonal cross frames to limit the lateral resistance to the framing action provided by the reinforced concrete deck, girders and chord members of the cross frames. Specimen F0A had the reinforced concrete deck connected to the top flanges of steel girders through headed stud connectors. Specimen F0B had the R/C deck connected to the top chord through headed stud connectors. These are the details recommended by the AASHTO Specifications to transfer the deck seismic forces to the bearings and substructures.

Test Setup

Figure 7 shows the elevation of the test setup that was designed to allow specimens to undergo lateral cyclic deformations. A hydraulic push–pull displacement-controlled actuator attached to the deck was used to apply the horizontal displacement. Both specimens were supported on ideal steel pins that allowed in-plane rotation and prevented any uplift.

Figure 8 is a photo of the test setup with specimen F0A where the test specimen, load cells, lateral support frames, actuator and the reaction blocks are shown. Lateral support frames were constructed around the specimens to prevent out-of-plane movement. Figure 9 shows the kinematic of the test setup for specimen F0A. As shown in this figure, the lateral displacement on the specimen produces double-curvature behavior in the top and bottom chords as well as rotational displacement demand at the studded joints over the girders top flanges.

Test Specimens

The width of the subassembly was 3 ft. The girders were spaced at 6 ft on centers, and the deck overhangs were 2.5 ft. The reinforced concrete deck was 4.5 in. thick with a haunch

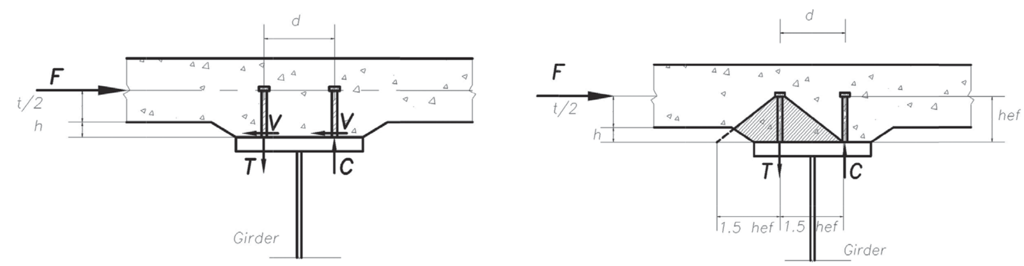

Fig. 6. (a) Seismic demands on stud connectors at supports; (b) concrete pull-out zone on the connector.

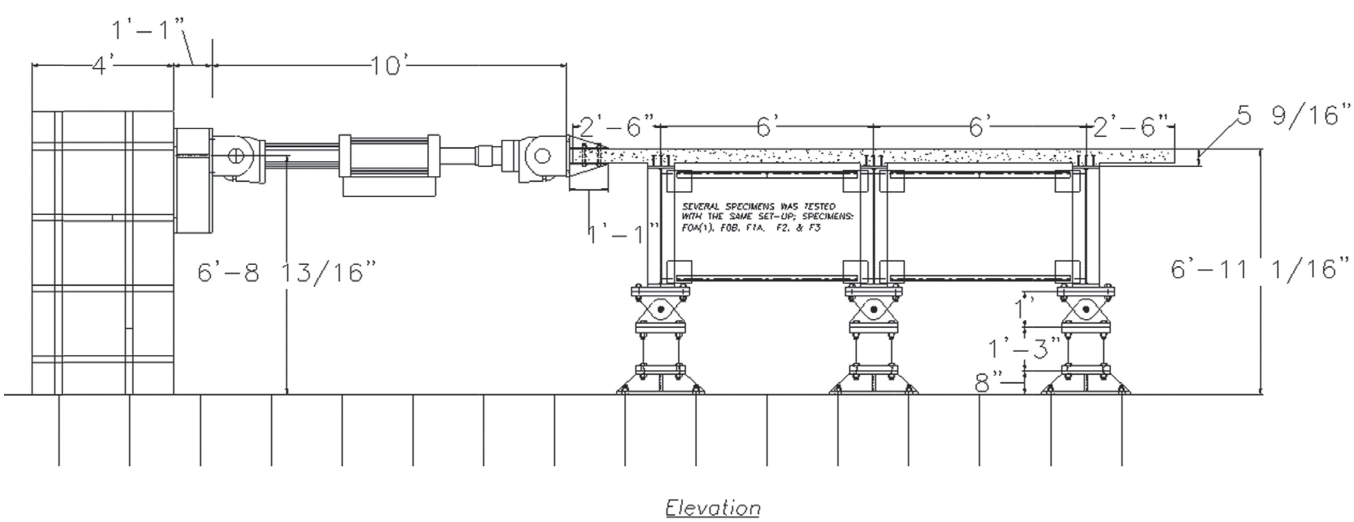

Fig. 7. Elevation and dimensions of test setup of specimen F0A.

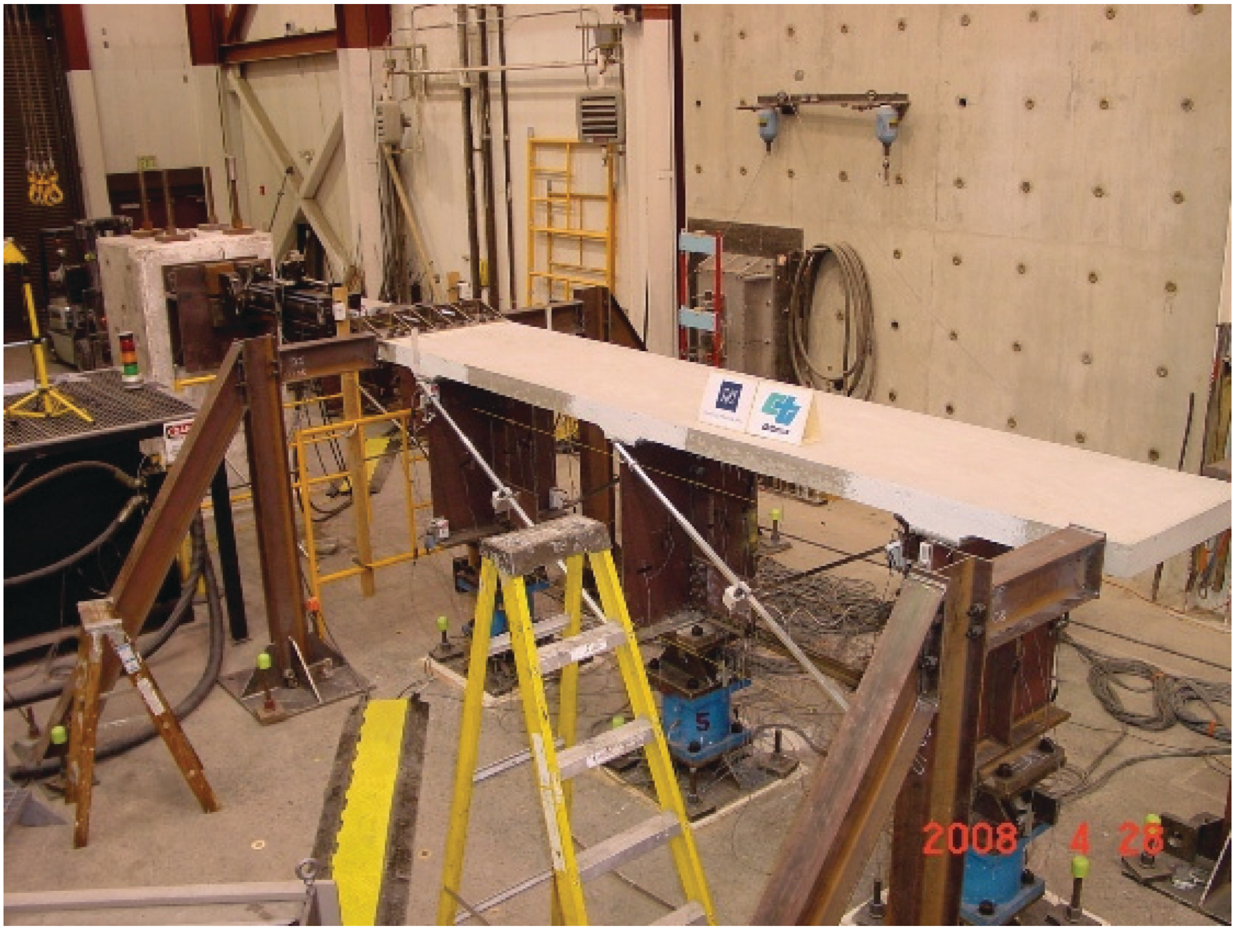

Fig. 8. Test setup inside the laboratory.

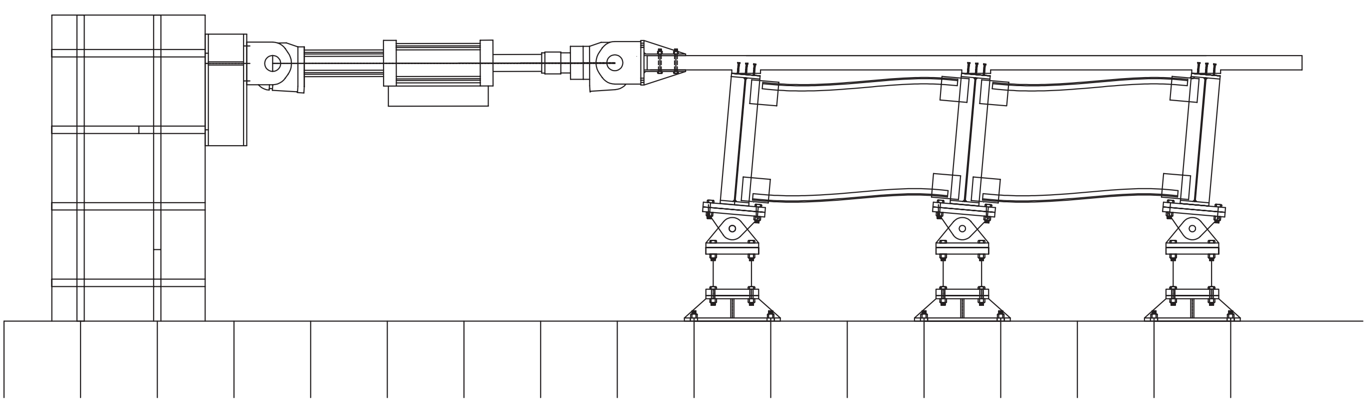

Fig. 9. Kinematics of the test setup for specimen F0A.

of 1.06 in. The deck longitudinal reinforcements were #3 at 8 in. and the transverse reinforcements were #3 at 5.5 in. The measured concrete strength was 4.0 ksi. The plate girders were built-up sections of 1-in.-thick by 9-in. flange plates and 5/16-in.-thick by 39-in. web plates. The bearing stiffener plates were 7/8 in. thick and 5 5/8 in. wide. The north, middle, and south girders of specimens and their corresponding reactions in the subassembly specimens are called girder 1, girder 2, and girder 3, respectively.

Specimen F0A

Figure 10 shows the dimensions and details of specimen F0A. The required number of stud connectors was calculated based on the AASHTO LRFD Bridge Design Specifications (AASHTO, 2008) using the shear capacity equations. The connectors used in the specimen were single-headed studs with a diameter of 3/8 in. and a total length of 3 9/16 in. The measured ultimate strength of the connectors was 80 ksi. The shear capacity of each connector was 6.6 kips, based on the AASHTO Specifications, using the actual strength of concrete and stud connectors. On each girder flange, over the bearing stiffeners or along the specimen centerline, three connectors spaced at 2 3/4 in. were provided. There were three connectors each row, and the spacing between each connector was 2 1/2 in. Additional rows of connectors were also provided at a distance 12 in. from the specimen centerline. Thus, the total shear resistance of the stud connectors was equal to 297 kips.

Specimen F0B

Figure 11 shows the details and dimensions of specimen F0B. As shown in Figure 11, the reinforced concrete deck dropped to the elevation of the top chords. The thickness of the deck in this region was 7 9/16 in. with a width of 12 in. The longitudinal reinforcements in this region were #3 bars spaced at 8 in., while the transverse reinforcements were #3 spaced at 5.5 in. In this specimen, no stud connectors were provided on the top flanges near the specimen centerline. The connectors were placed on the double-angle top chord, as shown in Figure 11. On each angle, 7 connectors spaced at 6 in. were provided; thus a total of 14 connectors connect the top chord to the reinforced concrete deck. Additional rows of connectors were also provided on the girder top flange at a distance 12 in. from the specimen centerline. Thus, the lateral resistance of the stud connectors was equal to 304 kips, based on the AASHTO Specifications and using the actual strength of concrete and connectors.

Loading Sequence

A displacement-controlled loading sequence was used for all experiments. This loading was adapted from the loading history for qualifying cyclic tests of buckling restrained braces as specified in Appendix T of the AISC *Seismic Provisions* (AISC, 2005). The specimen was subjected to two cycles at every specified drift level, as shown in Figure 12. The drift level was calculated based on the differential lateral displacement between the top and bottom flanges of the steel plate girders. Because the actuator force was applied at

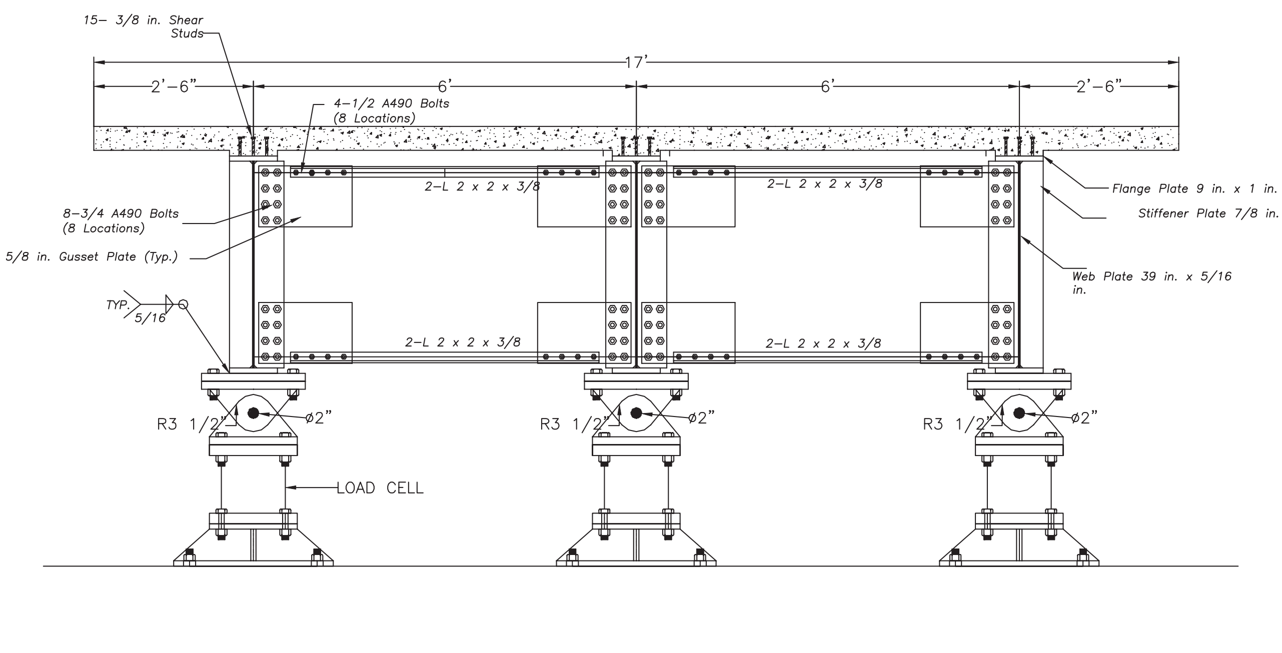

Fig. 10. Details of specimen F0A.

the deck level, the displacements that were measured from one of the diagonal displacement transducers were used to calculate the drift levels and fed into the actuator control program.

Cyclic Response of Specimen F0A

Figure 13 shows the lateral cyclic load-displacement response of the specimen in terms of total force versus the differential transverse displacement between the top and bottom flanges of the plate girders. The test showed that the ultimate, lateral load-carrying capacity of the specimen was 30 kips, and the lateral drift capacity was 6%. The elastic lateral stiffness of the specimens was 74 kips/in. The hysteresis loops show good energy dissipation capability. This is the result of the formation of plastic moment hinges at the ends of the top and bottom chords, which in turn was due to the framing action among the girders, reinforced concrete deck and chord members.

Experimental Observations

Flexural transverse cracks were developed across the deck near the girders at 1.5% drift. At 2% drift, a diagonal crack developed across the thickness of the concrete over girder 2, and the deck started to lift off from the top of the flange in this region. Further examination of the specimen after the test indicated that the concrete had failed in tension

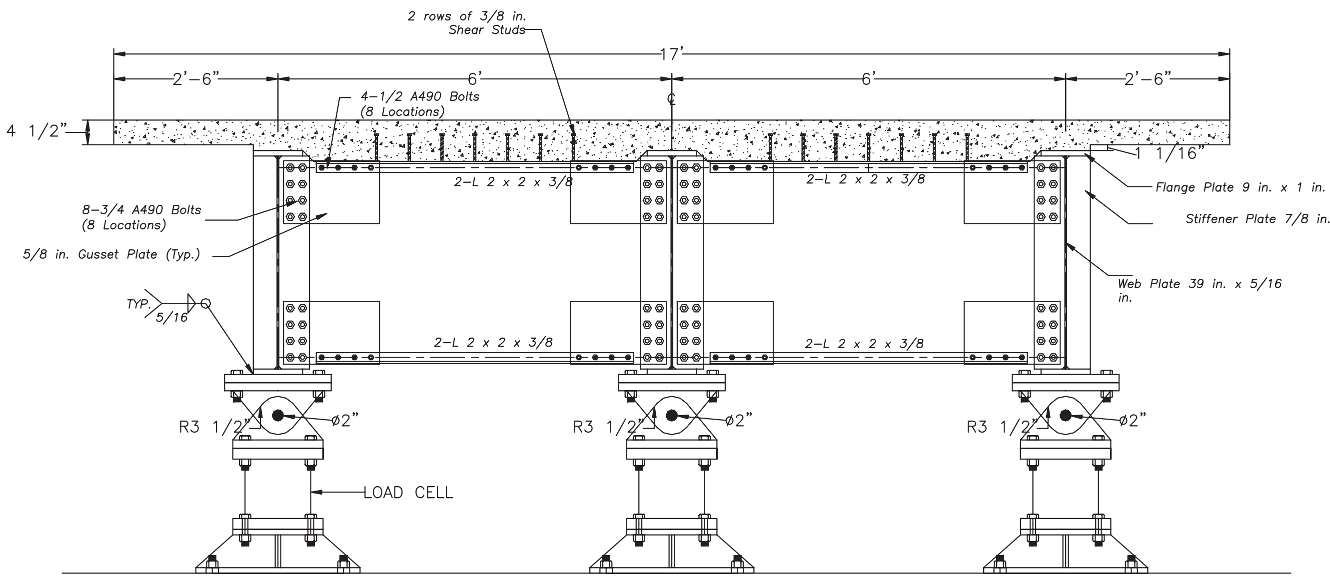

Fig. 11. Details of specimen F0B.

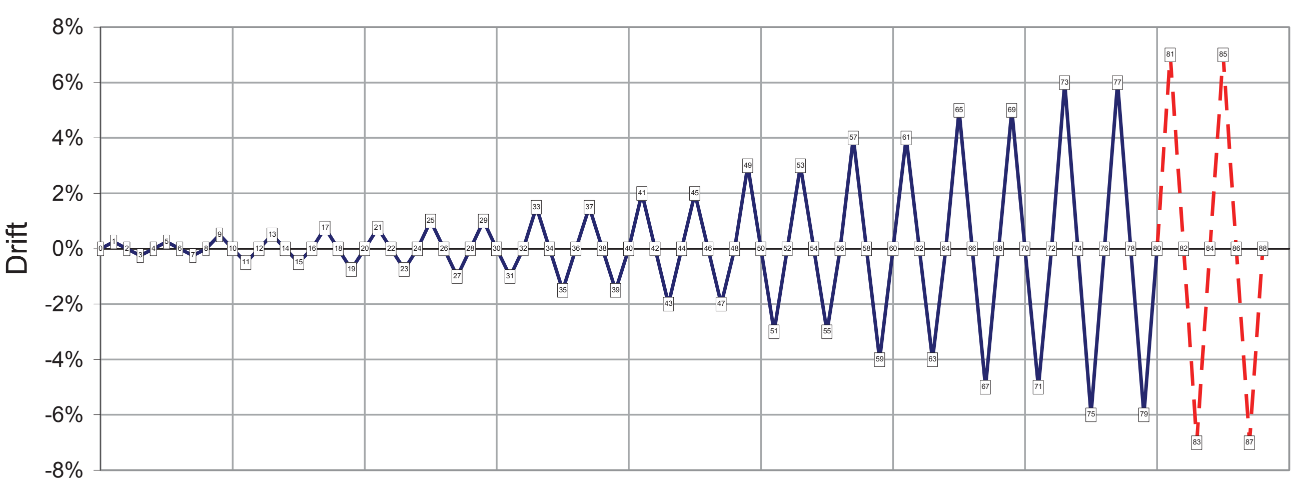

Fig. 12. Displacement-controlled loading sequence.

before the ultimate tensile strength of the stud connectors was reached. None of the connectors ruptured, but there was permanent axial deformation due to their yielding.

At 3% drift, diagonal cracks and uplift of the deck occurred over the flange of girder 1, while only slight deck separation was observed over girder 3. This indicated that at this drift level, the deck-girder joint connections over girders 1 and 2 had reached their ultimate capacity, while the full connection capacity was not yet developed over girder 3. This is evident in Figure 14, where the deformation and damage in Specimen F0A at 5% drift is shown.

Figure 15 shows the middle girder before and after the test. In addition to the diagonal cracks at the deck-girder joint connection, there was significant plastic deformation at the connections of the top and bottom chords to the gusset plates. The concrete breakout cones around the connector groups were visible during the deck demolition. At the end of the experiment, fractures were observed on the bottom chord at the first bolt-hole connection to the gusset plate. This is attributed to the low cycle fatigue due to high plastic strains in the angles near the connections.

Sequence of Yielding and Failure Modes

Figure 16 shows the envelope of base shear versus girder differential displacement. Examination of the strain gage data indicate that the ends of the chord members started to yield early on into the experiment at about 0.5% drift. The strains in the chords started to plateau between 1% to 1.5% drift. At this instance, the deck started to resist the lateral force through bending due to framing action with the girders, which led to the formation of visible flexural cracks in the deck. The strains in the chord increased at 1.5% to 2% drift as the connection between the deck and girder 2 fails. This caused redistribution of forces to girders 1 and 3.

Figure 17 shows the base shear plotted against the peak rotation of the deck-girder joints. This shows that the joint over girder 3 remained elastic up to 2% drift and experienced little nonlinearity before overall failure of the specimen occurred. The figure also shows that concrete joint over girders 1 and 2 underwent large rotations (0.05 rad.) before failure. Despite the failure of the concrete joint over girder 2 and its inability to transfer bending moments, the deck remained attached to the top flange of the girder 2 through the continuous bottom rebar mesh.

Cyclic Response of Specimen F0B

Figure 18 shows the lateral cyclic load-displacement response of specimen F0B in terms of total force versus the differential transverse displacement between the top and bottom flanges of the plate girders. The test showed that the ultimate, lateral load-carrying capacity of the specimen was 65 kips, the lateral drift capacity was 7% and the initial lateral stiffness of the specimens was 255 kips/in.

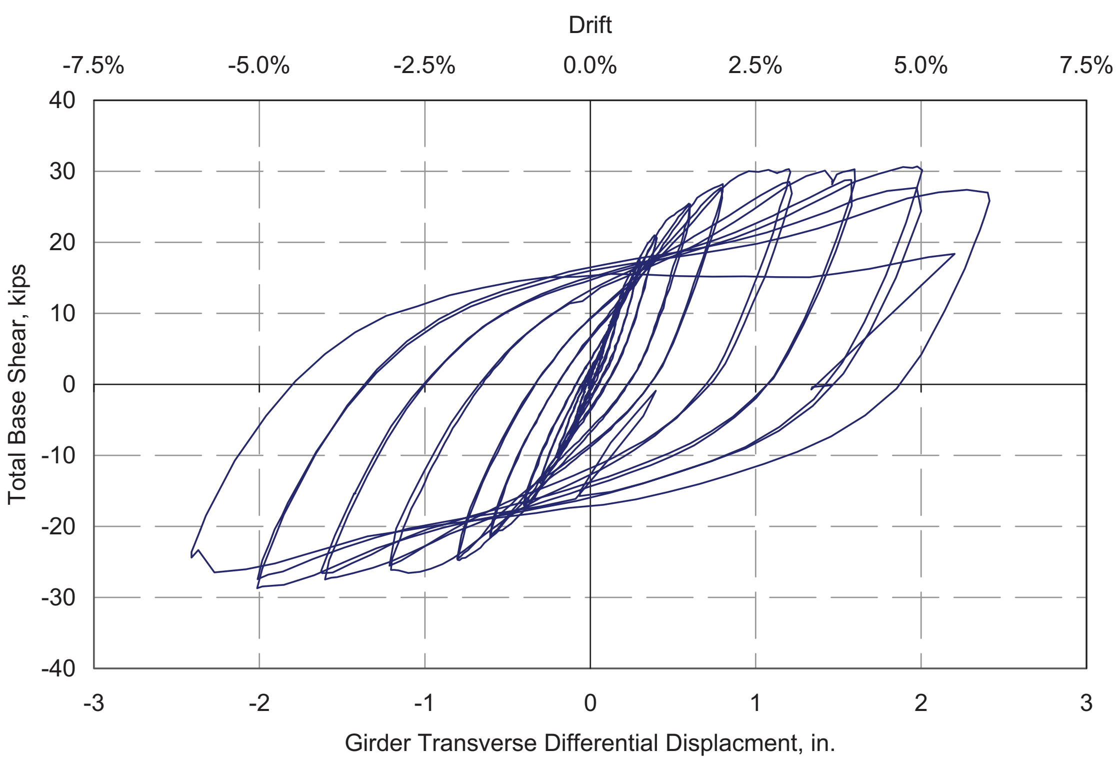

Fig. 13. Specimen F0A: actuator force versus girder differential displacement.

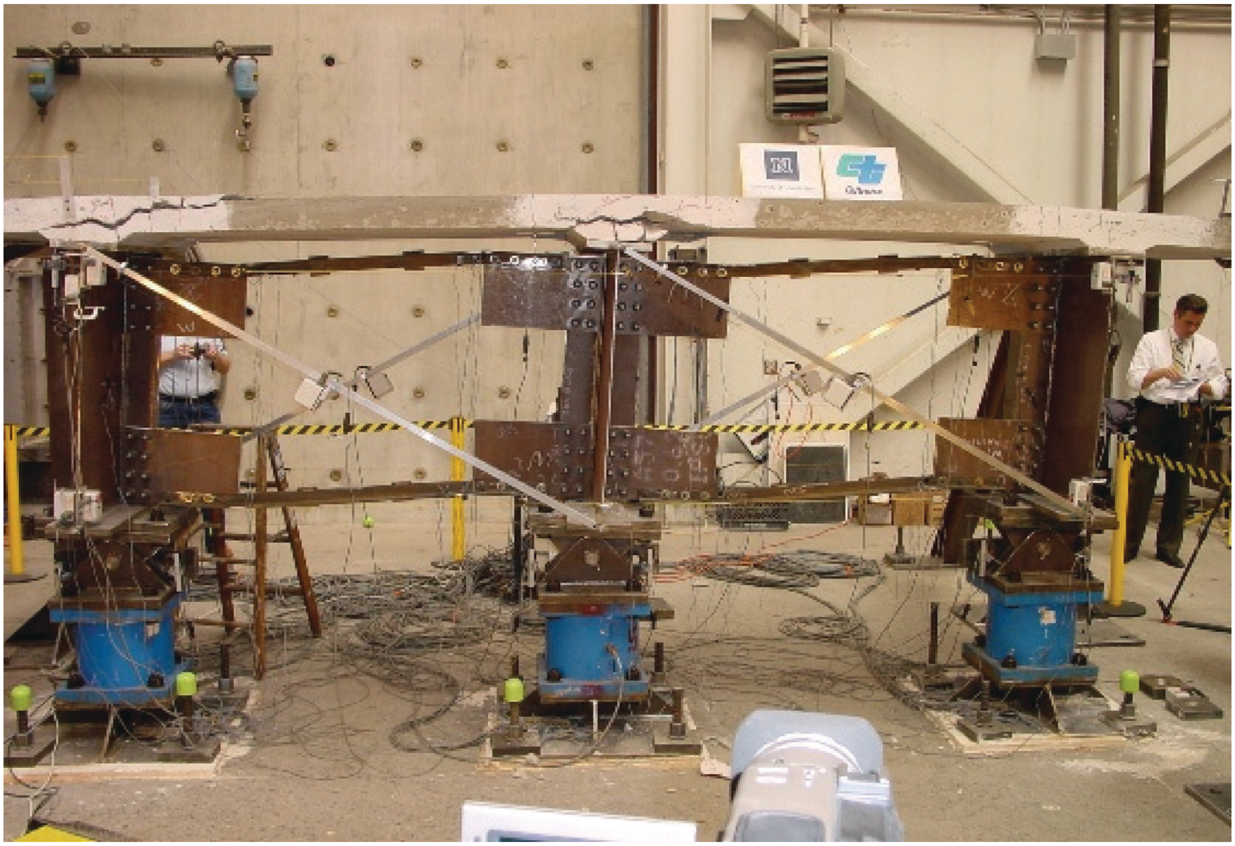

Fig. 14. Specimen F0A: deformation and damage at 5% drift.

Fig. 15. Specimen F0A: comparison of deformed and undeformed shape of middle girder (girder 2).

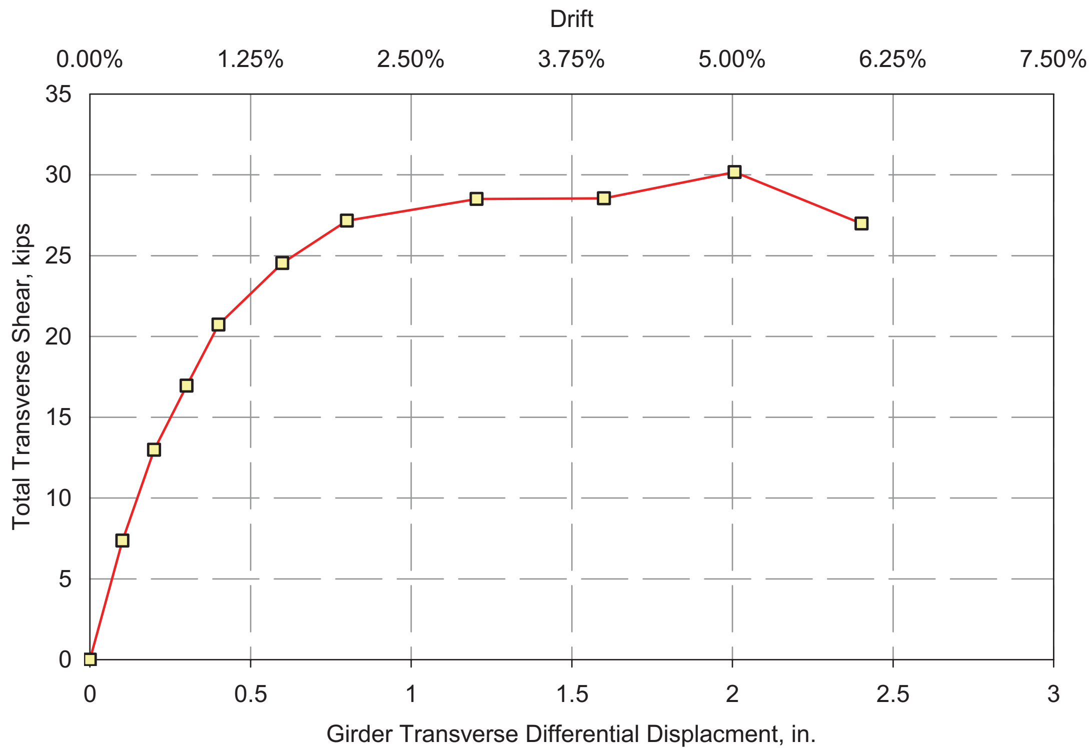

Fig. 16. Specimen F0A: base shear force-displacement plot.

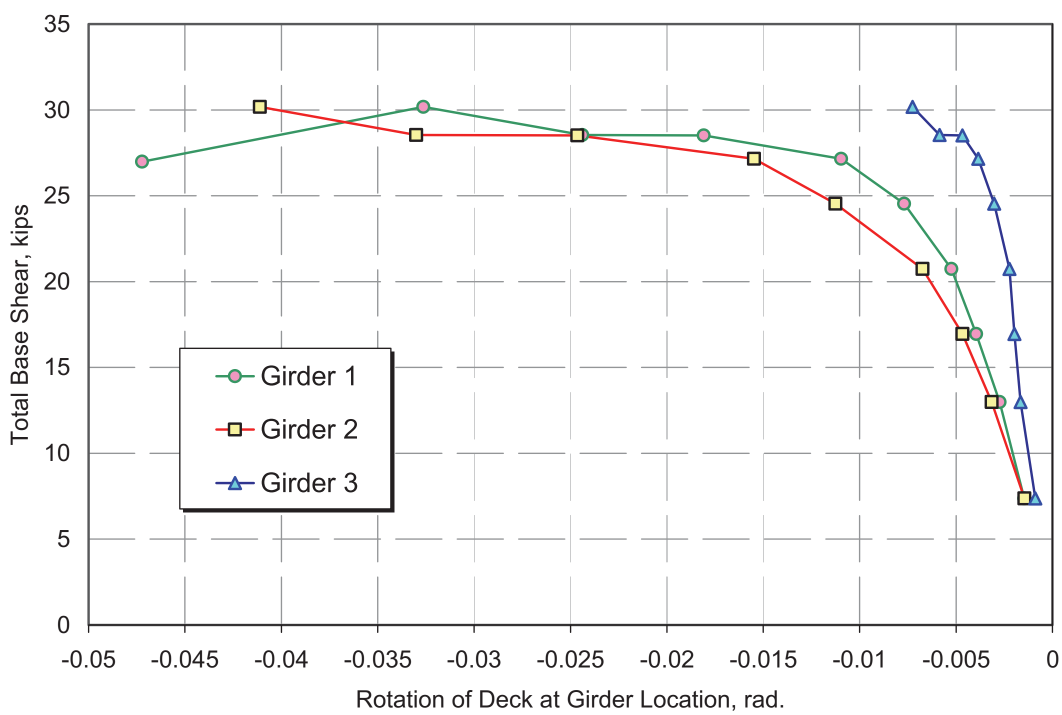

Fig. 17. Specimen F0A: base shear versus rotation of deck-girder joints.

Experimental Observations

Up to 0.75% drift, transverse cracks were developed across the deck. These cracks were due to flexural deformation of the deck. At 1% drift, cracks running north–south (i.e., in the direction of girder 1 to girder 3) on the deck surface were observed. At 1.5% drift, the ends of the chords showed separation from the concrete deck, indicating yielding of stud connectors in this area. At 2% drift, the deck-girder joint started to fail, and the deck started to separate (lift up) from the flanges of girders 2 and 3.

At 3% drift, the stud connectors close to the ends of the top chords ruptured due to high tension forces. Also, at this drift level, concrete breakout mode of failure started to occur in the deck-girder joint. High plastic rotation occurred at the ends of the chord members.

Figure 19 shows the deformation of specimen F0B at 6% drift. Vertical gaps (separations) and horizontal offsets between the underside of the deck and top flanges of the steel girders can be observed. Several factors contributed to this separation of the concrete deck and steel girder. This is attributed to the failure of stud connectors over girder 2, which caused the entire deck to bend in a single curvature between girders 1 and 3.

Due to the relatively large flexural stiffness of the thickened reinforced concrete deck at the connection with the top chord, large rotations that were concentrated on the top chord occurred near the ends of this connection. Figure 20 shows the separation between the deck and top chord. This separation caused high axial forces in the exterior stud connectors (i.e., connectors that were close to the ends of the deck–top chord connection). As these connectors fail, the connectors next in line and closer to the middle of the chords started to pick up the unbalanced force. At the end of the test, all the stud connectors over the top chords were ruptured, and significant plastic deformation in the top chords was visible. Additionally, the top chords were ruptured at the location of the last bolt hole due to high plastic strain concentration and low cycle fatigue.

Sequence of Yielding and Failure Modes

Figure 21 shows the envelope of base shear force versus girder differential displacement. The specimen exhibited larger elastic stiffness and yield strength compared with specimen F0A. Examination of the strain gages indicated that the ends of the chord members started yielding at 0.5% drift. As the transverse displacement is increased, the strains in the chords also increased, with corresponding increase in lateral force. The lateral stiffness and strength of the specimen dropped significantly when the top chords started yielding. The significant drop in strength shown in Figure 21 was due to fracture of the chord members near the connection to the gusset plate and failure of the stud

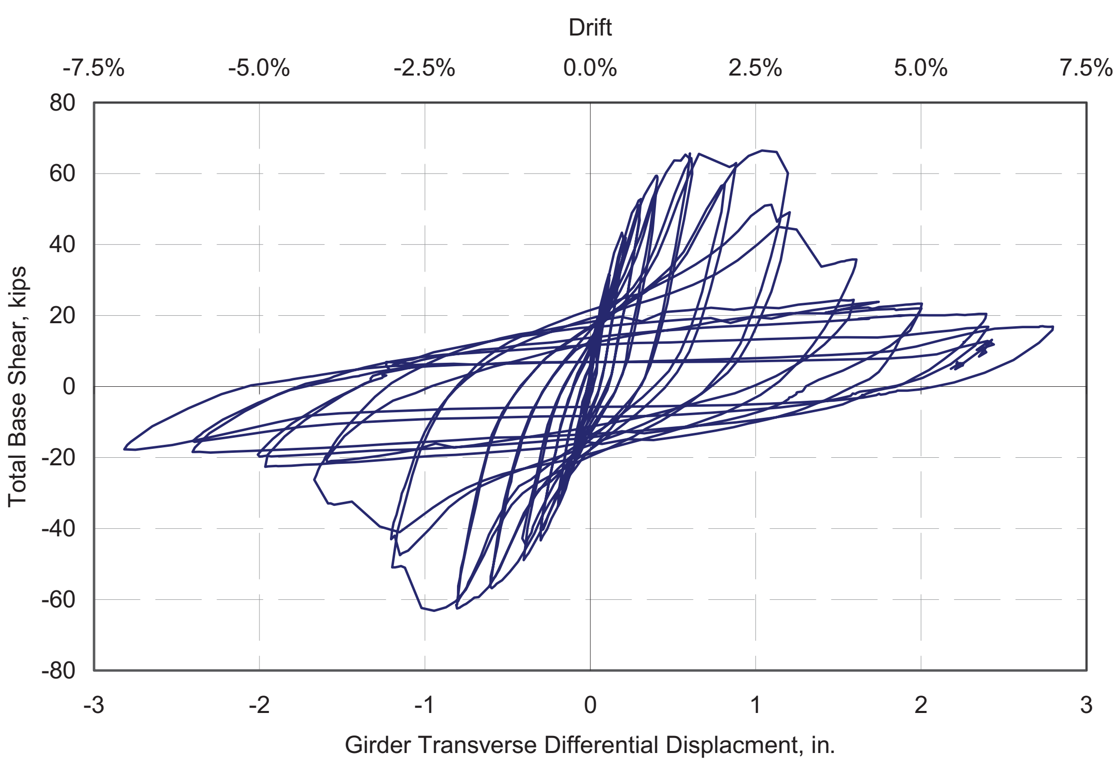

Fig. 18. Specimen F0B: actuator force versus girder differential displacement.

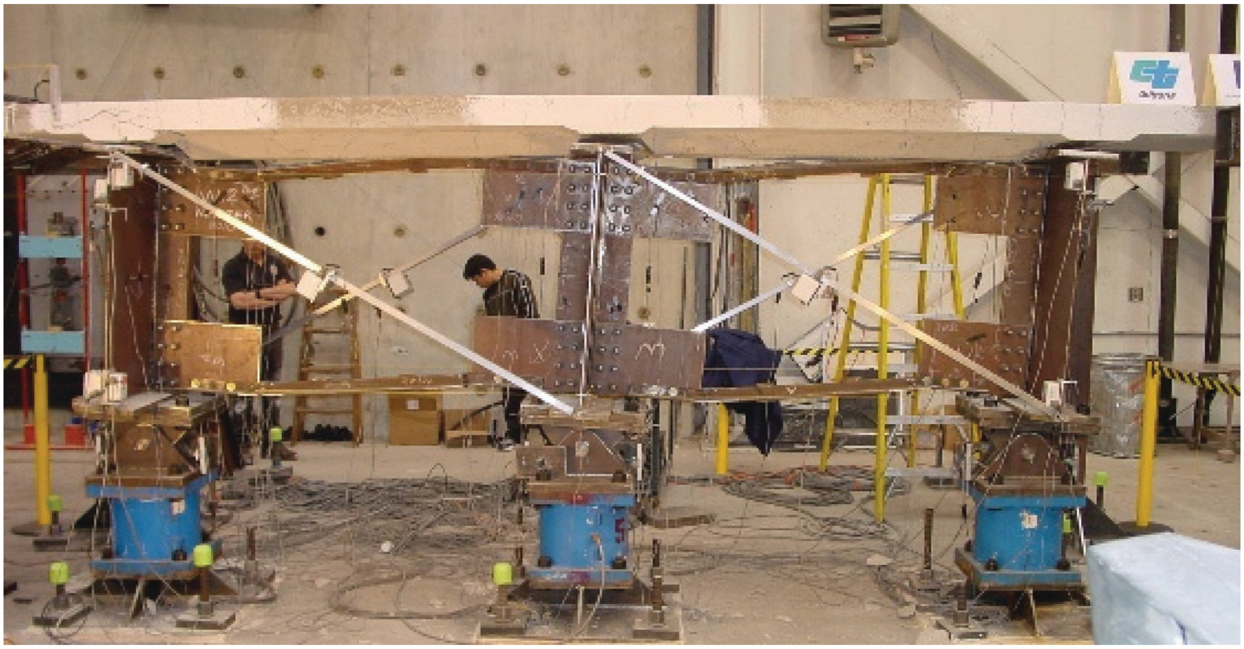

Fig. 19. Specimen F0B: deformed shape at 6% drift.

Fig. 20. Specimen F0B: rupture of stud connectors near the end of the top chord.

connectors. Although the specimen was able to resist higher lateral force and maintain higher lateral drift capacity, the deck experienced some damage.

LIMIT STATES OF TEST SPECIMENS

Based on these experiments, it was clear that stud connectors were subjected to combined shear and tension forces. Therefore, the interaction equation in Appendix D of ACI 318-08 (ACI, 2008) was used to better estimate their resistance under this combined loading. The strength of headed stud connector is given by:

$$\left(\frac{N_u}{N_r}\right)^{5/3} + \left(\frac{Q_u}{Q_r}\right)^{5/3} \leq 1.0 \tag{1}$$

where N_u is the seismic axial force demand per connector, Q_u is the seismic shear force demand per connector, N_r is the factored tensile capacity of a single connector and Q_r is the factored shear capacity of a connector. The tensile capacity is determined based on the lesser of stud connector ultimate axial capacity or concrete breakout capacity. The concrete breakout typically governs the design when the haunch is unreinforced. This can be improved by providing reinforcement around the stud connectors. This is evident in specimen F0B, where failure was due to stud fracture instead of concrete breakout. The ACI equations were used to determine the lateral strength of both specimens.

Specimen F0A

The lateral resistance of specimen F0A can be evaluated by dividing the subassembly into two framing systems: (1) the framing system formed by the deck and the girder and (2) the framing system formed by the chord members and the girders. The capacity in the first framing system is governed by the deck-girder joint connection capacity while, in the second, it is governed by moment capacities of the chord members.

A schematic diagram of lateral deformation of specimen 0A is shown in Figure 22. Based on the rotation of the deck-girder joint shown in Figure 22b, it can be assumed that one line of stud connectors is under compression while the other two lines are under tension. These sets of forces can, therefore, be used to calculate the moment in the connection. Using the ACI equations, the breakout strength of the group of connectors under tension is 38.9 kips. Because there are 10 connectors in this group, breakout strength of each connector is 3.9 kips. The tensile capacity of each connector is 8.8 kips. Therefore, the limit state of these connectors is based on concrete breakout, which is similar to the observed failure in the experiment. Based on 2.5-in.

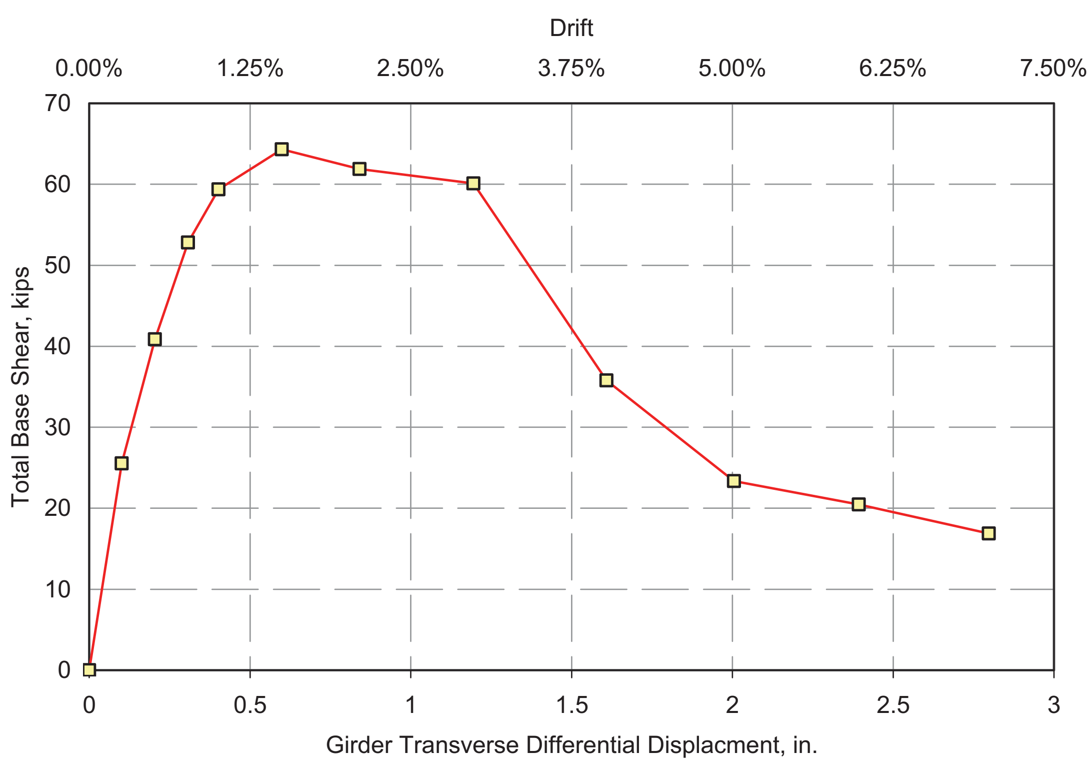

Fig. 21. Specimen F0B: base shear force-displacement plot.

transverse spacing between the connectors, the moment capacity of each deck-girder connection is equal to 145.9 kip-in. Because these moments act at the top of each girder, the lateral capacity provided by each connection can be calculated by dividing the moment capacity by the height from the top of girder to the centerline of the bearings, which is 48 in. The lateral capacity per girder is equal to 3.0 kips, and for the subassembly, it is equal to 9.0 kips.

The chord plastic moment capacity is 68 kip-in. based on a plastic section modulus of 1.27 in.^{3} and a measured yield strength of 54 ksi. The plastic hinges occur near the connection of the chord members to the gusset plates. The calculated lateral capacity due to the plastic moments is equal to 21.6 kips.

Therefore, the total lateral capacity of the subassembly based on combined capacity due to deck-girder frame action (9.0 kips) and chord-girder frame action (21.6 kips) is 30.6 kips. This calculated capacity closely match the experimental results of 30 kips as shown in Figure 16.

Specimen F0B

A schematic diagram of lateral deformation of specimen F0B is shown in Figure 23. The lateral force transfer mechanism in this model was mainly through the stud connectors connecting the deck to the top chord. The contribution of the deck-girder frame to the lateral capacity was considered negligible due to the small number of stud connectors on the girder top flange and because these connectors were placed 12 in. away from the centerline of subassembly as discussed previously. The degradation of the deck–top chord connection was due to high axial loads developed in the stud connectors, particularly at the ends of the connection, as illustrated in Figure 23b. In the experiment, it was observed that the limit state of the stud connectors at this location was fracture. This is because the connectors were subjected to large axial forces and deformations as the top chords deforms in flexure (Figure 23b).

The deck–top chord connection created a flexurally stiff composite section, which made specimen F0B stiffer than specimen F0A. It was shown in the experiment that the lateral stiffness of specimen F0B is more than three times the stiffness of specimen F0A.

Unlike in specimen F0A, a simplified model is not sufficient to evaluate the lateral capacity of specimen F0B due to distributed nonlinearity in the deck–top chord connection and flexural flexibility of the composite section of the top chord and deck. Therefore, a finite element model was developed to capture its response. Figure 24 shows the analytical model developed in SAP2000 (CSI, 2010). The deck, girders, stiffeners and gusset plates were modeled as shell elements while the stud connectors and chord members were modeled using frame elements. The connectors were modeled

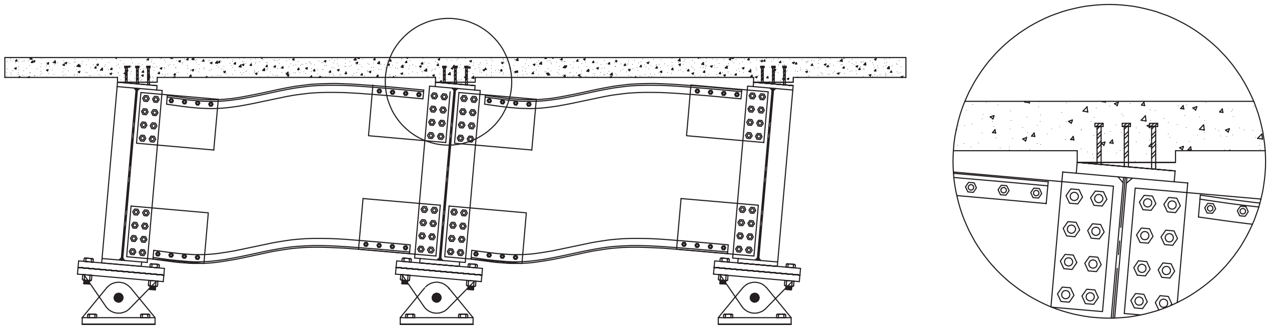
(a) (b)

Fig. 22. Specimen F0A: (a) deformed shape of subassembly; (b) rotation at deck-girder joint.

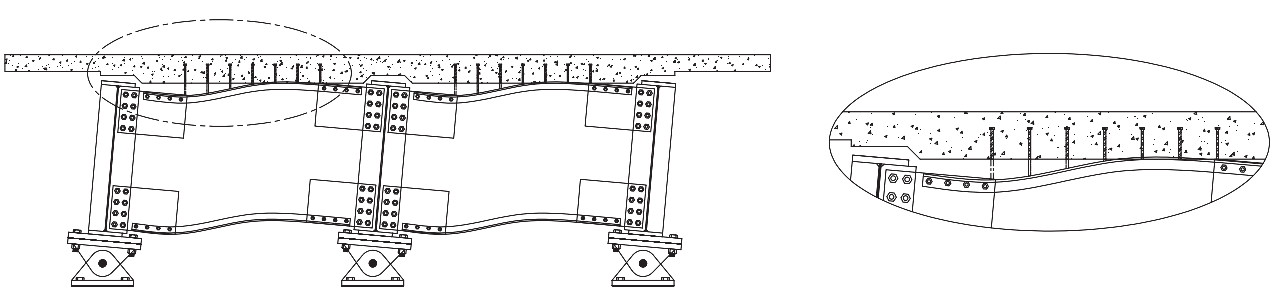

Fig. 23. Specimen F0B: (a) deformed shape of subassembly; (b) close-up of deformation at deck–top chord connection.

based on the truss analogy method developed by Bahrami, Itani and Buckle (2009). Plastic hinges were assigned to the chord elements near the connections. Figure 25 shows the pushover curve of the model compared with the envelope of base shear values at peak displacement cycles. The figure shows good correlation between the curves. The difference is attributed to the degradation of stiffness and strength in the deck–top chord connection.

SEISMIC DESIGN OF STEEL PLATE GIRDER SUPERSTRUCTURE

The findings of the preceding experiment, previous experimental and analytical investigations by other researchers and damage observed from earthquakes were used to develop a set of guidelines and specifications for seismic design of steel plate girder bridges (Itani, Grubb and Monzon, 2010). These have been adopted in the 2012 AASHTO LRFD Bridge Design Specifications (AASHTO, 2012) under the new Article 6.16, "Provisions for Seismic Design." These specifications concentrate on the seismic design and detailing of steel plate girder bridge superstructures. The common thread among these investigations was that these types of superstructures are vulnerable during earthquakes if they are not designed and detailed to resist the resulting seismic forces. A continuous and clearly defined load path is necessary for the transmission of the superstructure inertia forces to the substructure. The new specifications cover the design and detailing of reinforced concrete deck, stud connectors and cross frames and their connections.

SUMMARY AND CONCLUSIONS

Analytical investigations performed on steel plate girder superstructures showed that stud connectors are subjected to combined axial tensile and shear forces during seismic events. These forces are particularly large at the support locations, where the superstructure seismic forces are transferred to the substructure. As such, these connectors, if not designed properly, may fail prematurely during large earthquakes, altering the load path and subjecting other bridge components—such as intermediate cross frames—to forces for which they were designed. To verify this observation, two half-scale models of subassembly representing the deck, girder and chord members at the supports were constructed and subjected to cyclic testing. The test specimens represented two different configurations of transferring the deck seismic forces to the bearings and substructures: (1) the deck is connected to the girder top flange, and (2) the deck is connected to the top chords of the cross frames. Based on this study, the following observations and conclusions can be made:

- Stud connectors at support locations are essential in transferring the seismic forces to the cross frames.
- Seismic forces subject the stud connectors at support locations to combined axial tension and shear forces.
- Connecting the deck to the top chord at the supports increased the lateral stiffness and lateral strength of steel plate girder superstructure.

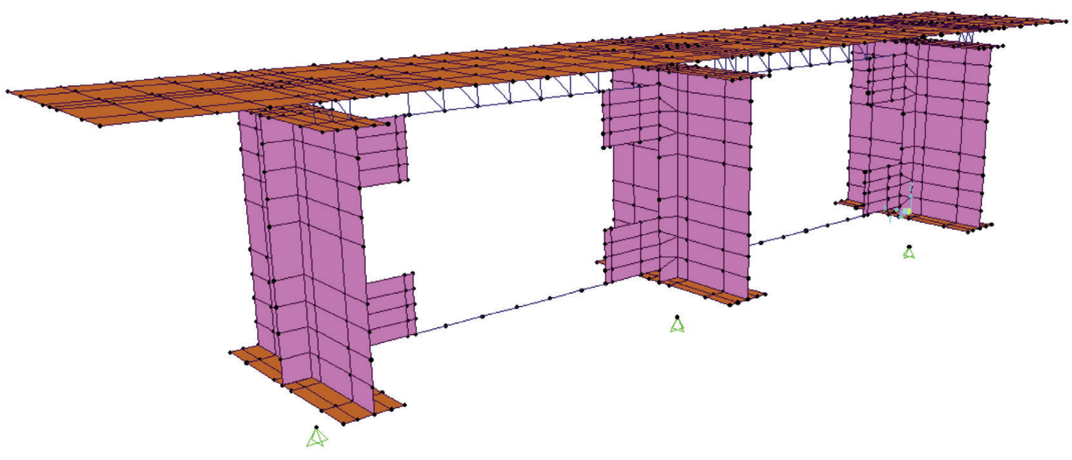

Fig. 24. Finite element model of specimen F0B.

- Interaction equation for stud connector resistance adopted in the new Article 6.16, "Provisions for Seismic Design," of the 2012 AASHTO LRFD Bridge Design Specifications must be used in seismic design of the connection between the reinforced concrete deck and the steel plate girder superstructure.

These observations and conclusions apply only to steel girder bridges with a drop cap. For steel girder bridges with an integral pier cap connection, design of stud connectors at the support is not required. The deck seismic forces are transferred directly from the deck to the concrete diaphragm and then to the substructure.

REFERENCES

AASHTO (2008). *AASHTO LRFD Bridge Design Specifications*, American Association of State Highway and Transportation Officials (AASHTO), Washington, DC.

AASHTO (2012). *AASHTO LRFD Bridge Design Specifications*, American Association of State Highway and Transportation Officials (AASHTO), Washington, DC.

ACI (2008). *Building Code Requirements for Structural Concrete (ACI 318-08) and Commentary*, American Concrete Institute (ACI), Farmington Hills, MI.

AISC (2005). *Seismic Provisions for Structural Steel Buildings*, American Institute of Steel Construction (AISC), Chicago, IL.

Bahrami, H., Itani, A.M. and Buckle, I.G. (2009). "Guidelines for the Seismic Design of Ductile End Cross-Frames in Steel Girder Bridge Superstructures," CCEER Report No. 09-04, Center for Civil Engineering Earthquake Research, University of Nevada, Reno, NV.

Caltrans (1992). "PEQIT Report-Highway Bridge Damage—Petrolia Earthquakes No. 1, No. 2, No. 3. of April 25–26, 1992," California Department of Transportation (Caltrans), Sacramento, CA.

Caltrans (2007). *Steel Girder Bridge Design Example,* AASHTO-LRFD, 3rd ed., with California Amendments, California Department of Transportation (Caltrans), Sacramento, CA.

Carden, L.P., Itani, A.M. and Buckle, I.G. (2005). "Seismic Load Path in Steel Girder Bridge Superstructures," CCEER Report No. 05-03, Center for Civil Engineering Earthquake Research, University of Nevada, Reno, NV.

CSI. (2010). SAP2000, Computers and Structures Inc., Berkeley, CA.

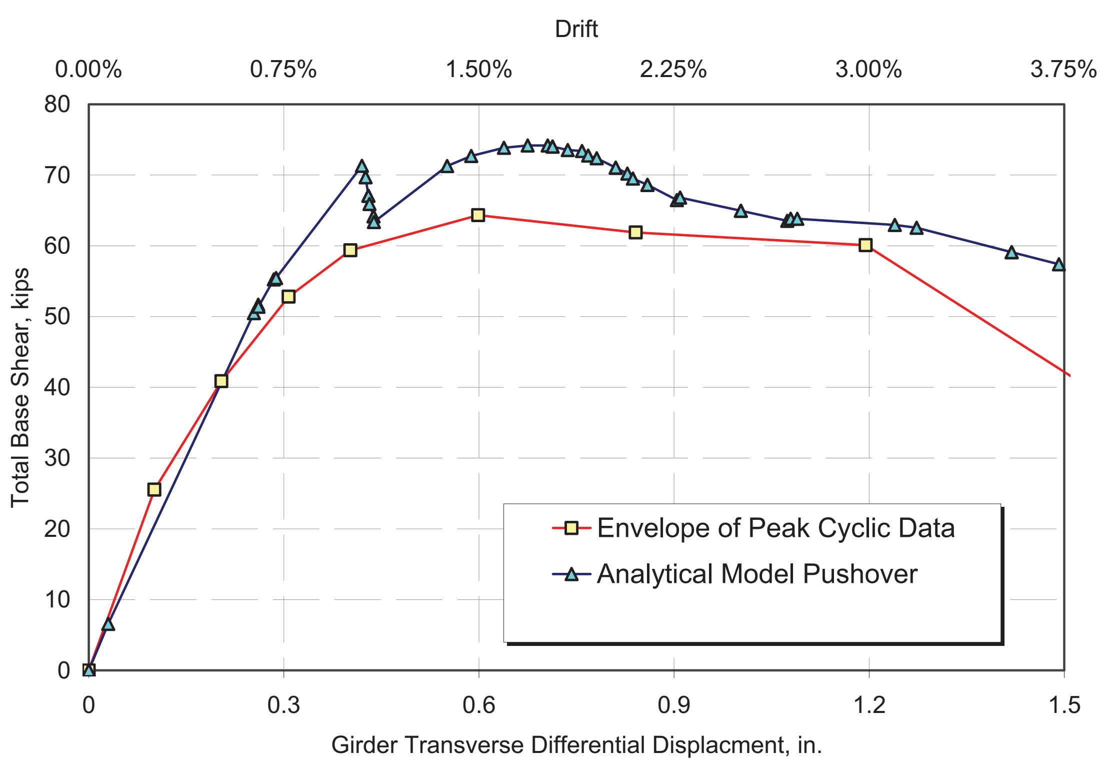

Fig. 25. Comparison of specimen F0B analytical model pushover result and experiment.

Gattesco, N. and Giuriani, E. (1996). “Experimental Study on Stud Shear Connectors Subjected to Cyclic Loading,” *Journal of Constructional Steel Research*, Vol. 38, no. 1, pp. 1–21.

Hawkins, N.M. and Mitchell, D. (1984). “Seismic Response of Composite Shear Connections,” *Journal of Structural Engineering*, Vol. 110, pp. 2120–2136.

Itani, A.M., Grubb, M. and Monzon, E.V. (2010). “Proposed Seismic Provisions and Commentary for Steel Plate Girder Superstructures,” CCEER Report No. 10-03, Center for Civil Engineering Earthquake Research, University of Nevada, Reno, NV.

Lloyd, R.M. and Wright, H.D. (1990). “Shear Connection between Composite Slabs and Steel Beams,” *Journal of Constructional Steel Research,* Vol. 15, No. 4, pp. 255–285.

McMullin, K.M. and Astaneh-Asl, A. (1994). “Cyclic Behavior of Welded Shear Studs,” *Proceedings of Structures Congress XII*, Atlanta, GA. April 24–28.

Mouras, J.M., Sutton, J.P., Frank, K.H. and Williamson, E.B. (2008). “The Tensile Capacity of Welded Shear Studs,” Report 9-5498-R2, Center for Transportation Research at the University of Texas, Austin, TX.

Oehlers, D.J. (1995). “Design and Assessment of Shear Connectors in Composite Bridge Beams,” *Journal of Structural Engineering*, Vol. 121, No. 2, pp. 214–224.

Oehlers, D.J. and Johnson, R.P. (1987). “The Strength of Stud Shear Connections in Composite Beams,” *The Structural Engineer*, Vol. 65B, No. 2, pp. 44–48.

Ollgaard, J.G., Slutter R.G. and Fisher, J.W. (1971). “Shear Strength of Stud Connectors in Lightweight and Normal-Weight Concrete,” *Engineering Journal*, AISC, Vol. 8, pp. 55–64.

Seracino, R., Oehlers, D.J. and Yeo, M.F. (2003). “Behavior of Stud Shear Connectors Subjected to Bi-Directional Cyclic Loading,” *Advances in Structural Engineering*, Vol. 6, No. 1, pp. 65–75.